Title

Hematopoietic Expression of Oncogenic BRAF Promotes Aberrant Growth of Monocyte-Lineage Cells Resistant to PLX4720

Journal

Molecular Cancer Research, 11(12)

ISSN

1541-7786

Authors

Kamata, Tamihiro
Dankort, David
Kang, Jing
et al.

Publication Date

2013-12-01

DOI

10.1158/1541-7786.mcr-13-0294

Peer reviewed

Published in final edited form as:
Mol Cancer Res. 2013 December ; 11(12): . doi:10.1158/1541-7786.MCR-13-0294.

Hematopoietic expression of oncogenic *BRAF* promotes aberrant growth of monocyte-lineage cells resistant to PLX4720

Tamihiro Kamata[1,2], **David Dankort**[3,4], **Jing Kang**[1], **Susan Giblett**[2], **Catrin A. Pritchard**[2], **Martin McMahon**[3], and **Andrew D. Leavitt**[1]

[1]Department of Laboratory Medicine, University of California, San Francisco, CA, USA

[2]Department of Biochemistry, University of Leicester, Leicester, United Kingdom

[3]Cancer Research Institute and Department of Cell and Molecular Pharmacology, Helen Diller Family Comprehensive Cancer Center, University of California, San Francisco, CA USA

[4]Department of Biology, McGill University, Montreal, QC, Canada

Abstract

Mutational activation of *BRAF* leading to expression of the $BRAF^{V600E}$ oncoprotein was recently identified in a high percentage of specific hematopoietic neoplasms in monocyte/histiocyte and mature B-cell lineages. Although $BRAF^{V600E}$ is a driver oncoprotein and pharmacological target in solid tumors such as melanoma, lung and thyroid cancer, it remains unknown whether $BRAF^{V600E}$ is an appropriate therapeutic target in hematopoietic neoplasms. To address this critical question, we generated a mouse model expressing inducible $BRAF^{V600E}$ in the hematopoietic system, and evaluated the efficacy of pathway-targeted therapeutics against primary hematopoietic cells. In this model, $BRAF^{V600E}$ expression conferred cytokine-independent growth to monocyte/macrophage-lineage progenitors leading to aberrant *in vivo* and *in vitro* monocyte/macrophage expansion. Furthermore, transplantation of $BRAF^{V600E}$-expressing bone marrow cells promoted an *in vivo* pathology most notable for monocytosis in hematopoietic tissues and visceral organs. *In vitro* analysis revealed that MEK inhibition, but not RAF inhibition, effectively suppressed cytokine-independent clonal growth of monocyte/macrophage-lineage progenitors. However, combined RAF and PI3K inhibition effectively inhibited cytokine-independent colony formation, suggesting autocrine PI3K pathway activation. Taken together, these results provide evidence that constitutively activated $BRAF^{V600E}$ drives aberrant proliferation of monocyte-lineage cells. This study supports the development of pathway-targeted therapeutics in the treatment of $BRAF^{V600E}$-expressing hematopoietic neoplasms in the monocyte/histiocyte lineage.

Keywords

$BRAF^{V600E}$; Monocytosis; Pathway-targeted therapeutics; Mouse model

Corresponding author: Andrew D Leavitt, MD, Department of Laboratory Medicine, University of California, San Francisco, 513 Parnassus Ave, Room S-561, San Francisco, CA 94143-0100, USA. Phone: 415-514-3432; Fax: 415-514-3433; leavitta@labmed2.ucsf.edu..

The online version of the article contains a data supplement.

Conflict of Interest Disclosure The authors declare no competitive financial interests. M.M. acknowledges research support from Glaxo-Smith-Kline, Novartis, Pfizer & Plexxicon.

Europe PMC Funders Author Manuscripts

Introduction

Somatic mutations in *BRAF* are detected in a wide variety of human cancers, most notably melanoma, colon, lung and thyroid cancer (1). The most common mutation observed in 90% of *BRAF*-mutated cancers is a T1799→A transversion in exon 15 of *BRAF*, which results in expression of $BRAF^{V600E}$ (2). In hematopoietic malignancies, *BRAF* mutations were initially reported infrequently (3-7), and the majority involved non-V600 residues except for therapy-related acute monocytic leukemia (5). However, recent reports of *BRAF* mutation in a high percentage of human hairy cell leukemia (HCL) (8), Langerhans cell histiocytosis (LCH) (9) and Erdheim-Chester disease (ECD) (10) highlights the potential importance of the $BRAF^{V600E}$ oncoprotein in specific types of hematopoietic neoplasms.

Mutationally activated $BRAF^{V600E}$ is a constitutively active protein kinase that activates the MEK1/2→ERK1/2 pathway (11, 12). Enhanced MEK→ERK pathway signaling is therefore thought to drive $BRAF^{V600E}$-related neoplastic transformation, and indeed, it has been shown in animal models that MEK→ERK activation is the major driving force for $BRAF^{V600E}$-induced tumorigenesis in lung tumors and melanoma (13, 14). However, although *in vitro* studies have implicated a role for the BRAF→MEK→ERK pathway in multiple stages of myelopoiesis (15) and the terminal differentiation of erythroblasts (16), the *in vivo* relevance of these findings to hematopoietic neoplasms remains unknown. A previously reported mouse model using the interferon-inducible promoter Mx1 to conditionally activate $BRAF^{V600E}$ expression demonstrated skin lesions consistent with histiocytic sarcoma (17). However, early post-natal lethality precluded detailed characterization of hematopoietic organs in those transgenic mice on a C57BL/6 background (17).

Consistent with previous analysis of genetically engineered mouse (GEM) models, (14), RAF inhibitors vemurafenib and dabrafenib, and a MEK inhibitor trametinib, have proven their clinical efficacy against $BRAF^{V600E}$-expressing metastatic melanoma (18-20). However, limited efficacy of vemurafenib due to feedback activation of EGFR has been also reported for some types of $BRAF^{V600E}$-expressing solid cancers especially colorectal and thyroid cancers (21-23), suggesting that the sensitivity of $BRAF^{V600E}$-expressing tumors to RAF inhibitors may vary among tissue types. In hematopoietic neoplasms expressing $BRAF^{V600E}$, sporadic cases with HCL (24) or ECD/LCH (25) responding to short-term treatment with vemurafenib have been reported, but their overall and long-term efficacy in large cohorts has yet to be proven by randomized controlled clinical trials. Development of relevant animal models is essential for the appropriate design of such clinical trials and further drug development.

To advance our understanding of the pathology of $BRAF^{V600E}$-related hematopoietic disorders, we crossed $Braf^{CA/+}$ mice (13) with *Mx1::Cre* mice (26) to generate *Mx1::Cre;* $Braf^{CA/+}$ mice on a mixed C57/Bl6/FVBN background (referred to as "$BRAF^{V600E}$" mice in this manuscript). These mice survived ≥5 weeks, circumventing the previously reported early post-natal lethality (17), thereby enabling us to characterize $BRAF^{V600E}$-induced aberrant hematopoiesis in primary animals, *in vitro* culture of hematopoietic tissue from primary mice, and adoptive transfer of $BRAF^{V600E}$ bone marrow into sublethally-irradiated recipients. $BRAF^{V600E}$-expressing mice developed a monocyte-predominant leukocytosis with thrombocytopenia, anemia, and early lethality. $BRAF^{V600E}$-expressing bone marrow recipients demonstrated monocyte expansion in hematopoietic tissues with visceral organ involvement. With primary hematopoietic tissue readily available, we were able to demonstrate that $BRAF^{V600E}$ expression confers cytokine-independent growth on monocyte-lineage progenitors, which can be suppressed by MEK inhibition but not by the RAF inhibitor, PLX4720. We also show that the inability of the PLX4720 to prevent

BRAF^{V600E}–driven cell autonomous growth is explained, at least in part, by autocrine activation of the PI3′-kinase signaling pathway. Our data provide novel insights into the pathogenesis of BRAF^{V600E}-expressing hematopoietic neoplasms, suggesting that MEK inhibitors may play an important role in the treatment of such disorders and that RAF inhibitors in isolation may have limited utility, and the mouse model offers a platform for pre-clinical development and validation of pathway-targeted therapeutics against BRAF^{V600E}-expressing hematopoietic neoplasms of the monocyte/histiocyte lineage.

Materials and methods

Mice

The generation and genotyping of *Braf*^{CA} allele were previously described (13). *Braf*$^{CA/+}$ mice on a FVBN background were crossed with the *Mx1::Cre* strain (26) on a C57BL/6 background, generating *Mx1::Cre;Braf*$^{CA/+}$ (BRAF^{V600E}) mice on the mixed background. *Braf*$^{CA/+}$ littermates lacking the *Mx1::Cre* transgene were used as controls. Some mice were intraperitoneally injected with 250μg of polyinosine-polycytidylic acid (poly I:C) at 3 weeks of age. *Rag2*$^{-/-}\gamma c^{-/-}$ mice (27) were purchased from the Jackson Laboratory. Biochemical analyses were performed in part using BRAF^{V600E}-expressing mice on a pure C57BL/6 background (17). All animal procedures were approved and performed in accordance with UCSF animal care guidelines or under UK Home Office License authority.

Cell Line

The SigM5 cell line (28) was purchased from DSMZ (German Collection of Microorganisms and Cell Cultures) and maintained in IMDM supplemented with 20% heat-inactivated FCS with splitting saturated cultures at 1:2 every 3-4 days. The heterozygous *BRAF*^{T1799A} mutation in this cell line was confirmed by sequencing exon 15.

Hematopoietic cell isolation

Cells were obtained from peripheral blood by retro-orbital puncture, or from tissues by passing through a 70μm-nylon mesh. Bone marrow was harvested from hind limbs using standard procedures.

Pathological analysis

Complete blood counts were obtained using a HEMAVET HV850 (CDC Technologies) hematology analyzer. Blood smears and bone marrow cytospins were stained with Diff-Quick (Baxter). For histological analyses, tissues fixed in 10% neutral-buffered formalin were embedded into paraffin, sectioned and stained with hematoxylin-eosin at the UCSF Comprehensive Cancer Center Core Facility. Immunohistochemistry was performed as previously descried (17).

Flow cytometry analysis and cell sorting

1×10^6 cells or circulating leukocytes from 20μl blood were incubated on ice for 5min with anti mouse Fc-receptor antibody (BD Biosciences), stained for 45min with a panel of fluorochrome-conjugated antibodies against Mac1, Gr1, CD71, TER119, CD19, and CD3 (BD Biosciences), and analyzed using FACSCalibur and CellQuest software (BD Biosciences). Cells stained with anti-Gr1 and Mac1 antibodies were sorted using a MoFlo (DakoCytomation) machine.

Colony-forming assays

Colony forming assays were performed as described (15, 29). Human EPO (Ortho Biotech), human TPO (Genentech), mouse SCF (Peprotech), mouse IL-3 (Peprotech), and/or mouse

GM-CSF (Peprotech) were supplemented. Genomic DNA was extracted from developed colonies as described (15).

Bone marrow transplantation

Donor cells were prepared by pooling bone marrow nucleated cells from 2 $BRAF^{V600E}$ or control mice at 3 weeks after poly I:C injection, and 2×10^6 cells per recipient mouse were injected into sub-lethally-irradiated (5Gy) *Rag2*$^{-/-}\gamma c^{-/-}$ mice on a C57BL/6 background through retro-orbital venous plexus. Some recipients were injected only with PBS to confirm the recovery of host hematopoiesis after sub-lethal irradiation.

Immunoblotting

Protein lysates were prepared and analyzed by SDS-PAGE as previously described (30). Primary antibodies used were: anti-BRAF (Santa Cruz #sc-5284), anti-CRAF (BD Biosciences #610152), anti-ERK2 (Santa Cruz #sc-1647), anti-phospho ERK1/2 (Cell Signaling #9101), anti-phospho AKT (S473) (Cell Signaling #4060), anti-phospho CRAF (S338) (Cell Signaling #9427) and anti-AKT (Cell Signaling #4691) antibodies.

In vitro liquid culture and drug treatment

Primary mouse bone marrow cells expanded in DMEM+10%FCS for 5 days were transferred into serum-free DMEM with or without inhibitors, and cultured for 24-96 hours before protein harvest. Conditioned media was collected after 96hr serum-free cultures, and used to stimulate the cells starved for serum for 5 hrs. SigM5 cells plated at 5×10^5/ml in IMDM+20%FCS were treated with inhibitors for 6 days, and viable cell numbers were manually counted by trypan blue dye exclusion every 3 days. PD0325901 and PI-103 were purchased from Cayman Chemical, and PLX4720 from Selleck Chemicals.

Statistics

Comparison between any two groups was performed by Student's t-test for normally distributed data, or by non-parametric Mann-Whitney test for non-normally distributed data.

Results

Leukocytosis, anemia, thrombocytopenia and lethality in $BRAF^{V600E}$ mice

Our murine model employs a Cre-activated *Braf* allele (*Braf*^{CA}) that allows for expression of normal BRAF prior to the activity of Cre recombinase, after which $BRAF^{V600E}$ is expressed in a tissue-specific manner from its normal chromosomal locus at physiologically relevant levels (13). We expressed Cre recombinase from the inducible Mx1 promoter, which is activated by synthetic double stranded RNA (poly I:C). However, extensive recombination of the *Braf*^{CA} allele occurred spontaneously by three weeks of life without poly I:C injection leading to early demise in both poly I:C injected and uninjected *Mx1::Cre; Braf*^{CA} mice (Fig. 1A). Essentially complete recombination of the conditional *Braf*^{CA} allele was observed in hematopoietic tissues in the absence of poly I:C injection (Fig. 1B), indicating a substantial growth advantage for hematopoietic cells expressing $BRAF^{V600E}$.

Given the spontaneous recombination, the known pro-inflammatory activity of poly I:C, and an observed impact of poly I:C on enhancing leukocytosis (data not shown), we performed the remaining experiments on mice not injected with poly I:C to remove it as a confounding variable.

We first analyzed peripheral blood to begin to understand the hematopoietic pathology in the $BRAF^{V600E}$ mice. $BRAF^{V600E}$ mice developed a significant and progressive leukocytosis,

thrombocytopenia, and anemia by 3 weeks of age (Fig. 1C-D). Surface marker and morphological analyses of circulating leukocytes in the absence of poly I:C was most notable for a marked expansion of monocytes ($Mac1^+Gr1^-$) in addition to neutrophilia ($Mac1^+Gr1^+$) in the $BRAF^{V600E}$ mice (Fig. 1E & 1F).

Deregulated myelopoiesis and erythropoiesis in $BRAF^{V600E}$ spleen and bone marrow

The $BRAF^{V600E}$ mice died with massive splenomegaly (Fig. 2A). The spleens of $BRAF^{V600E}$ mice contained markedly increased $Mac1^+$ myeloid and $TER119^+$ erythroid cells and relatively decreased lymphocytes compared with controls (Fig. 2B), and follicular structures were effaced (Fig. S1A). The majority of splenic $TER119^+$ erythroid cells from these mice co-expressed CD71 at a high level (Fig. 2C), indicating maturation arrest at the early basophilic erythroblast stage (31). Extramedullary hematopoiesis was also observed in the liver (Fig. S1B) and lung (Fig. S2).

Bone marrow investigation of the $BRAF^{V600E}$ mice revealed myeloid and erythroid cells at various stages of differentiation, and did not have morphologic evidence of overt leukemia. Surface marker analyses confirmed that $Mac1^+Gr1^{low/-}$ cells, mainly monocyte-lineage cells ($Mac1^+/Gr1^{low/-}$), were increased compared to controls (Fig. 2D-E). $TER119^+$ erythroid cells were not relatively increased (Fig. 2D), but there was relative maturation arrest at the erythroblast stage similar to what was found with splenic erythroblasts (Fig. 2E).

Cytokine-independent growth of $BRAF^{V600E}$ monocyte/macrophage-lineage progenitors

The *Mx1::Cre* transgene has known activity outside the hematopoietic compartment (26), consistent with some $BRAF^{V600E}$ mice developing lung papillary adenomas (Fig. S2), and alterations in non-hematopoietic tissues could affect the hematopoietic phenotype in a non-cell-autonomous manner. Therefore, to understand cell-autonomous characteristics of $BRAF^{V600E}$ hematopoietic cells, we first tested the growth of bone marrow cells in clonal *in vitro* cultures. In stark contrast to control bone marrow, $BRAF^{V600E}$ bone marrow cells readily developed myeloid colonies composed largely of macrophages, in the absence of cytokines (Fig. 3A), demonstrating that $BRAF^{V600E}$ confers cell-autonomous cytokine-independent growth and differentiation to monocyte/macrophage-lineage progenitors. Similar findings were observed using spleen cells from $BRAF^{V600E}$ mice (Fig. 3A).

In contrast to wild-type marrow cells that typically require SCF and EPO to generate erythroid colonies, marrow from $BRAF^{V600E}$ mice formed erythroid colonies with EPO as the sole supplemental cytokine (Fig. 3A). Cell sorting revealed that the cytokine-independent progenitors were detected almost exclusively in the $Mac1^-Gr1$-population from $BRAF^{V600E}$ bone marrow (Fig. 3B and S3). While control bone marrow progenitors demonstrated a clear dose-response for increased colony formation with increasing cytokine concentrations, colonies in the mutant bone marrow culture were only modestly increased with increasing IL-3 or GM-CSF (Fig. 3C). Although the colony size was much larger for progenitors from the mutant mice than control mice at suboptimal cytokine concentrations (Fig. S4), the size and number of the mutant colonies were not increased at high cytokine concentrations (Fig. 3C, data not shown). When cultured with a broad spectrum of cytokines, IL-3 (10ng/ml), SCF (50ng/ml), EPO (4U/ml) and TPO (100ng/ml), the $BRAF^{V600E}$ bone marrow cells generated significantly fewer colonies than controls (Fig. 3D). In contrast, colony-forming activity was significantly increased in the spleen (Fig. 3D), suggesting redistribution of progenitors as part of the extramedullary hematopoiesis observed in the $BRAF^{V600E}$ mice. Cytokine-independent growth of $BRAF^{V600E}$-expressing bone marrow cells was also observed in bulk liquid culture, with initial development of $Mac1^+Gr1^{low/-}$ immature monocytic cells followed by differentiation into macrophages co-expressing a histiocyte marker CD11c (Fig. S5).

Monocytosis, anemia, thrombocytopenia, and tissue infiltration in sub-lethally irradiated $BRAF^{V600E}$ bone marrow transplant recipients

To further understand the cell-autonomous nature of the $BRAF^{V600E}$-expressing bone marrow cells, we performed adoptive transfer of primary bone marrow cells into sub-lethally-irradiated mice. We utilized immune-deficient *Rag2*$^{-/-}\gamma c^{-/-}$ mice (27) as recipients to circumvent graft rejection given the mixed background of our $BRAF^{V600E}$ mice. Circulating leukocyte counts in $BRAF^{V600E}$ marrow recipients were increased relative to sham transplant recipients, but not to the same extent as control marrow recipients (Fig. 4A). However, in marked contrast to control marrow, circulating leukocytes of $BRAF^{V600E}$ marrow recipients was composed predominantly of $Mac1^{+}Gr1^{-}$ monocytic cells (Fig. 4B). Recipients of control marrow demonstrated a lymphoid predominant engraftment as evident by the increased circulating Mac1-negative leukocytes (Fig 4B), as would be expected for wild-type marrow engrafting into an immunodeficient recipient.

Interestingly, progressive anemia and thrombocytopenia were observed in recipients of $BRAF^{V600E}$ marrow, a finding in marked contrast to animals transplanted with control marrow, and to sham control animals that underwent the same sublethal irradiation but did not receive any donor cell infusion (Fig. 4A). The $BRAF^{V600E}$ marrow recipients also demonstrated marked splenomegaly (Fig. 4C), and a relative increase of $Mac1^{+}Gr1^{low/-}$ monocytic cells in bone marrow and spleen (Fig. 4D). $TER119^{+}$ erythroid cells were increased in the spleen (Fig. 4D) where they were arrested at the erythroblast stage (Fig. 4E), similar to primary animals (Fig. 2C). The relative percentage of $Mac1^{+}Gr1^{high}$ granulocytes was not increased in $BRAF^{V600E}$ marrow recipients in either bone marrow or spleen (Fig. 4D).

We performed methylcellulose cultures of recipient bone marrow cells in the absence or presence of cytokines, and genotyped individual colonies. Cytokine-independent macrophage colonies were detected in 5 out of 6 $BRAF^{V600E}$ marrow recipients and none of the control recipients (Table 1). As expected, genotyping of randomly plucked colonies confirmed all to be of donor ($BRAF^{V600E}$) origin. When cultured in the presence of multiple cytokines, fewer colonies were detected in $BRAF^{V600E}$ transplant recipients than in transplanted control animals, similar to what was seen in the primary mice (Fig. 3D left). The level of donor chimerism in the colony-forming cells ranged from 0 to 93.3% among $BRAF^{V600E}$ recipients, and on average, the number of donor-derived bone marrow myeloid progenitors in $BRAF^{V600E}$ marrow transplant recipients was 23% of that seen in control recipients (Table 1; 19.1% vs. 82.6%). In contrast, myeloid colony forming activity in recipient spleens was markedly increased in all $BRAF^{V600E}$ recipients compared with control recipients (Fig. 4F). Residual, recipient-derived bone marrow progenitors in $BRAF^{V600E}$ marrow transplant recipients were also decreased relative to wild-type marrow recipients (62.6 vs. 110.8 colonies/1×10^{5} marrow leukocytes) despite the relatively lower donor-chimerism (Table 1), suggesting possible suppression of recipient progenitors by transplanted $BRAF^{V600E}$ bone marrow cells.

Histologic analysis of $BRAF^{V600E}$ marrow recipients demonstrated stellate nodular lesions in the lung (Fig. 5A) and periportal lesions in the liver (Fig. 5B) in all $BRAF^{V600E}$ marrow recipients examined. Both the liver and lung infiltrative lesions contained cells that stained positive for S100 expression (Fig. 5A vii-viii, and 5B iv), one of the immunohistological markers for diagnosis of human histiocytic/dendritic cell neoplasms including Langerhans cell and interdigitating dendritic cell tumors (32). The lung lesions sometimes displayed foamy histiocyte infiltration, characteristic of non-Langerhans cell type histiocytosis, which were also positive for S100 (Fig. S6A). In contrast to the lesions in visceral organs, marrow sections were largely negative for S100 (Fig. S6B).

In vitro sensitivity to pathway-targeted therapeutics

To investigate if MEK→ERK activity contributes to the aberrant growth of $BRAF^{V600E}$-expressing monocyte-lineage cells, we examined ERK phosphorylation in primary $BRAF^{V600E}$ bone marrow cells and the effects of MEK and RAF inhibitors on the cytokine-independent colony formation. As expected, robust ERK phosphorylation was detected in $BRAF^{V600E}$ cells compared to controls (Fig. 6A) and, consistent with its importance in cell proliferation, the MEK inhibitor PD0325901 effectively inhibited colony formation (Fig. 6B). In contrast, the RAF inhibitor PLX4720 failed to suppress spontaneous colony formation (Fig. 6B), which correlated with only partial inhibition of ERK phosphorylation (Fig. 6C). We hypothesized that PLX4720-resistance in the colony assay and in ERK phosphorylation could be mediated through intracellular feedback activation of cell surface receptors (21-23), or by extracellular stimuli through autocrine/paracrine mechanisms (33, 34) that in turn activate intracellular signaling pathways. To investigate this, we examined AKT and CRAF phosphorylation in $BRAF^{V600E}$-expressing bone marrow cells, and found hyperphosphorylation of both AKT and CRAF (Fig. 6D) in response to PLX4720. AKT hyperphosphorylation was detectable when stimulated with conditioned media (CM) from $BRAF^{V600E}$ bone marrow cells cultured in serum-free media in the absence of PLX4720, which was further enhanced by the addition of PLX4720 (Fig. 6E), suggesting that PLX4720 can augment intracellular signaling triggered by the secreted factors. The AKT hyperphosphorylation was not detected when the same experiments were performed using conditioned media from control bone marrow cells that do not express $BRAF^{V600E}$ (data not shown).

Increased AKT phosphorylation was also observed in the primary $BRAF^{V600E}$-expressing $Mac1^{-}Gr1^{-}$ bone marrow cells (Fig. 6F) enriched for the cytokine-independent progenitors (Fig. 3B), and pharmacological inhibition of PI3′-kinase by PI-103 suppressed cytokine-independent colony formation without affecting ERK phosphorylation (Fig. 6G), further supporting the biological significance of PI3′-kinase activation by secreted factors *in vivo* and *in vitro*. The combinatorial treatment with PI-103 sensitized the cytokine-independent marrow progenitors to PLX4720 (Fig. 6H), indicating the essential role of PI3′-kinase signaling in resistance to PLX4720 in this context. Consistent with these data, the $BRAF^{V600E}$ expressing human monoblastic SigM5 cell line (Supplemental Fig. 7) also demonstrated only modest growth inhibition by PLX4720 alone, but showed marked growth inhibition to a combination of PLX470 and PI-103 (Fig. 6I). Hepatocyte growth factor (HGF) signaling through the receptor c-MET has been shown to contribute to BRAF inhibitor resistance in $BRAF^{V600E}$-expressing solid cancers (33, 34). However, HGF levels in CM from $BRAF^{V600E}$ bone marrow cells was found to be substantially much lower than in control CM, and pharmacological inhibition of c-MET with crizotinib failed to effectively suppress CM/PLX4720-induced AKT phosphorylation (data not shown), which together suggesting that secreted factors other than HGF play a role in the RAF inhibitor resistance observed in our mouse model.

Discussion

Mutationally activated $BRAF^{V600E}$ and $KRAS^{G12D}$ oncoproteins are thought to drive hematopoietic cell transformation through sustained MEK→ERK activation. *RAS* mutations are frequently detected in human myeloid neoplasms (35), and cause myeloproliferative neoplasms (MPNs) in animal models (36-38). *In vivo* MEK inhibition ameliorates $KRAS^{G12D}$-induced MPN in mice (39), providing compelling evidence that MEK→ERK hyperactivation drives oncogenic $KRAS^{G12D}$-induced aberrant myelopoiesis. Accordingly, we began this study hypothesizing that Mx1::Cre-mediated induction of $BRAF^{V600E}$ expression would generate an MPN that is pathologically similar to oncogenic $KRAS^{G12D}$.

However, our findings show that BRAF^{V600E} promotes pathology distinct from KRAS^{G12D}-induced MPN. Although primary BRAF^{V600E} mice displayed leukocytosis and splenomegaly reminiscent of RAS models (36-42), our analysis, including pathology in the primary mice, *in vitro* analysis and adoptive transfer of BRAF^{V600E} expressing bone marrow cells revealed aberrant monocytosis as the primary phenotype elicited by BRAF^{V600E}. Pulmonary involvement in our primary and transplant models, together with skin histiocytic tumors in primary animals previously reported (17), distinguishes the BRAF^{V600E} model from previous RAS models. In contrast to the KRAS^{G12D} transplant model in which MPN was reproduced in all recipients injected with a large number of hematopoietic stem cells (40), most recipients in our transplant model do not exhibit marked leukocytosis, despite monocyte-dominant reconstitution observed in peripheral blood, marrow and spleen. These phenotypic characteristics contrast with classic murine MPN models. Moreover, while our model confirms some aspects of BRAF^{V600E}-induced monocyte/histiocyte-lineage neoplasms in human (5, 9, 10), the prolonged life span allowed for extensive hematologic analysis, transplantation and in vitro cultures to identify cell-autonomous characteristics, and adequate hematologic tissue to identify critical observations relevant to the future development of molecularly-targeted therapy for BRAF^{V600E}-activated hematologic neoplasms.

Cytokine-independent colony formation is commonly observed in RAS MPN models (38, 41, 42) as well as our BRAF model, suggesting that aberrant ERK activation is a key event for the cytokine-independent growth of myeloid progenitors. Nevertheless, adoptive transfer of unfractionated bone marrow produced distinct outcomes; RAS models develop T-cell malignancies in addition to MPNs (39, 40, 42), while our model yields neither. Biochemical analysis of BRAF^{V600E}-expressing bone marrow cells revealed constitutive ERK phosphorylation, not observed in bone marrow progenitors in RAS models (38, 41). Such strong ERK activation may perturb lymphopoiesis by inhibiting lymphoid-lineage commitment (43), resulting in the failure to develop overt lymphoid neoplasms including HCL, another hematopoietic neoplasm in which the *BRAF^{T1799A}* mutation is frequently found (8). Although BRAF^{V600E} may contribute to the development of B-cell neoplasms after a longer latency, rapid progression of the fatal myeloid disease in our model did not allow us to determine long-term consequences of BRAF^{V600E} expression in the B-lymphoid lineage. This hypothesis needs to be tested by crossing *Braf$^{CA/+}$* mice with B-lineage specific Cre strains to develop HCL models.

Our functional and biochemical analysis of BRAF^{V600E}-expressing bone marrow cells treated with PLX4720 demonstrate that BRAF^{V600E}-expressing monocyte-lineage progenitors display incomplete MEK→ERK pathway inhibition leading to sustained proliferation in the presence of the drug. Consistent with previous studies using hematopoietic cell lines with conditional RAF or MEK activation (44, 45), BRAF^{V600E}-expressing monocyte-lineage cells secrete autocrine factors that activate PI3′-kinase, and presumably other pathways not assessed herein, which contribute to the cytokine-independent growth of monocyte-lineage progenitors. Moreover, autocrine activation of PI3′-kinase signaling appears to be further enhanced by PLX4720, quite possibly through receptor tyrosine kinase activation as reported for colorectal cancer cells (21). However, our initial analysis ruled out a contribution of the HGF/c-MET signaling axis (data not shown). Since RAS activation by autocrine factors can lead to the “paradoxical activation” of CRAF activation in the presence of PLX-4720 (46, 47), this may contribute to the residual ERK activity in PLX4720-treated cells. In contrast, the suppression of recipient-derived bone marrow progenitors in our transplant model (Table 1) suggests that paracrine factors secreted by donor-derived monocyte-lineage cells in the bone marrow could inhibit residual wild-type hematopoiesis. The virtual absence of mature erythroblasts in the spleen (Fig. 4E) also suggests that differentiation of not only BRAF^{V600E} expressing but also recipient-

derived wild-type erythroblasts could be blocked by non-cell-autonomous mechanisms. Thus, secreted factors by $BRAF^{V600E}$ monocyte-lineage cells may not only promote RAF inhibitor resistance in an autocrine manner, but also interfere with normal hematopoiesis in a paracrine manner at progenitor and erythroblast levels to cause progressive bi-lineage cytopenia in our $BRAF^{V600E}$ marrow recipients.

While our data imply that human monocyte-lineage progenitors expressing the $BRAF^{V600E}$ oncoprotein may be similarly resistant to RAF inhibitors, a recent clinical study has reported the efficacy of vemurafenib on three ECD patients carrying the $BRAF^{T1799A}$ mutation (25). Our data showing AKT hyperphosphorylation specifically in the $Mac1^{-}Gr1^{-}$ population in $BRAF^{V600E}$ marrow *in vivo* suggests that PLX4720-resistance through PI3′-kinase pathway activation may specifically occur in the progenitor population, and that *BRAF*-mutated monocyte-lineage progenitors, potentially resistant to RAF inhibitors, may not be involved in the pathogenesis of human ECD. However, the apparent clinical efficacy during the short-term treatment does not guarantee the drug's effectiveness on tumor-initiating populations, which may be more resistant than mature progeny and cause disease resistance or reactivation during ongoing therapy. If *BRAF*-mutated monocyte-lineage progenitors resistant to RAF inhibitors are the pathogenic precursors for ECD or aggressive forms of LCH, RAF inhibitors may have limited long-term efficacy against these diseases. In such cases, regimens of RAF inhibitors combined with inhibition of either MEK1/2 or PI3′-kinase might be considered as alternative therapeutic options. Indeed, "vertical" combined inhibition of both $BRAF^{V600E}$ and MEK1/2 has already demonstrated clinical efficacy against BRAF mutated melanoma (48). Our model provides a valuable platform for preclinical evaluation of novel pathway-targeted therapeutic approaches against *BRAF*-mutated monocyte/histiocyte-lineage neoplasms.

Supplementary Material

Refer to Web version on PubMed Central for supplementary material.

Acknowledgments

We thank Shuwei Jiang for cell sorting, Eric Morse and Yimdriuska Magan for excellent technical assistance, including mouse handling, and Martin JS Dyer and Jesvin Samuel for providing the SigM5 cell line.

This work was supported by National Institutes of Health grant HL54476 (A.D.L.), the General Motors Cancer Research Scholars Program (D.D.), Mouse Models of Human Cancer Consortium CA084244, RO1 CA131261, and U.C. Discovery Grant (M.M.), and Cancer Research UK program grant C1362/A6969 (C.A.P.).

Financial Support: This work was supported by National Institutes of Health grant HL54476 (A.D.L.), the General Motors Cancer Research Scholars Program (D.D.), Mouse Models of Human Cancer Consortium CA084244, and U.C. Discovery Grant (M.M.), and Cancer Research UK program grant C1362/A6969 (C.A.P.).

References

1. Kamata T, Pritchard C. Mechanisms of aneuploidy induction by RAS and RAF oncogenes. Am J Cancer Res. 2011; 1:955–971. [PubMed: 22016838]
2. Davies H, Bignell GR, Cox C, Stephens P, Edkins S, Clegg S, et al. Mutations of the BRAF gene in human cancer. Nature. 2002; 417:949–954. [PubMed: 12068308]
3. Gustafsson B, Angelini S, Sander B, Christensson B, Hemminki K, Kumar R. Mutations in the BRAF and N-ras genes in childhood acute lymphoblastic leukaemia. Leukemia. 2005; 19:310–312. [PubMed: 15538400]
4. Lee JW, Soung YH, Park WS, Kim SY, Nam SW, Min WS, et al. BRAF mutations in acute leukemias. Leukemia. 2004; 18:170–172. [PubMed: 14603338]

5. Christiansen DH, Andersen MK, Desta F, Pedersen-Bjergaard J. Mutations of genes in the receptor tyrosine kinase (RTK)/RAS-BRAF signal transduction pathway in therapy-related myelodysplasia and acute myeloid leukemia. Leukemia. 2005; 19:2232–2240. [PubMed: 16281072]
6. Lee JW, Yoo NJ, Soung YH, Kim HS, Park WS, Kim SY, et al. BRAF mutations in non-Hodgkin's lymphoma. Br J Cancer. 2003; 89:1958–1960. [PubMed: 14612909]
7. Chapman MA, Lawrence MS, Keats JJ, Cibulskis K, Sougnez C, Schinzel AC, et al. Initial genome sequencing and analysis of multiple myeloma. Nature. 2011; 471:467–472. [PubMed: 21430775]
8. Tiacci E, Trifonov V, Schiavoni G, Holmes A, Kern W, Martelli MP, et al. BRAF mutations in hairy-cell leukemia. N Engl J Med. 2011; 364:2305–2315. [PubMed: 21663470]
9. Badalian-Very G, Vergilio JA, Degar BA, MacConaill LE, Brandner B, Calicchio ML, et al. Recurrent BRAF mutations in Langerhans cell histiocytosis. Blood. 2010; 116:1919–1923. [PubMed: 20519626]
10. Haroche J, Charlotte F, Arnaud L, von Deimling A, Hélias-Rodzewicz Z, Hervier B, et al. High prevalence of BRAF V600E mutations in Erdheim-Chester disease but not in other non-Langerhans cell histiocytoses. Blood. 2012; 120:2700–2703. [PubMed: 22879539]
11. Mercer KE, Pritchard CA. Raf proteins and cancer: B-Raf is identified as a mutational target. Biochim Biophys Acta. 2003; 1653:25–40. [PubMed: 12781369]
12. Garnett MJ, Marais R. Guilty as charged: B-RAF is a human oncogene. Cancer Cell. 2004; 6:313–319. [PubMed: 15488754]
13. Dankort D, Filenova E, Collado M, Serrano M, Jones K, McMahon M. A new mouse model to explore the initiation, progression, and therapy of $BRAF^{V600E}$-induced lung tumors. Genes Dev. 2007; 21:379–384. [PubMed: 17299132]
14. Dankort D, Curley DP, Cartlidge RA, Nelson B, Karnezis AN, Damsky WE Jr, et al. $Braf^{V600E}$ cooperates with Pten loss to induce metastatic melanoma. Nat Genet. 2009; 41:544–552. [PubMed: 19282848]
15. Kamata T, Kang J, Lee TH, Wojnowski L, Pritchard CA, Leavitt AD. A critical function for B-Raf at multiple stages of myelopoiesis. Blood. 2005; 106:833–840. [PubMed: 15784729]
16. Zhang J, Lodish HF. Constitutive activation of the MEK/ERK pathway mediates all effects of oncogenic H-ras expression in primary erythroid progenitors. Blood. 2004; 104:1679–1687. [PubMed: 15166036]
17. Mercer K, Giblett S, Green S, Lloyd D, DaRocha Dias S, Plumb M, et al. Expression of endogenous oncogenic ^{V600E}B-raf induces proliferation and developmental defects in mice and transformation of primary fibroblasts. Cancer Res. 2005; 65:11493–11500. [PubMed: 16357158]
18. Chapman PB, Hauschild A, Robert C, Haanen JB, Ascierto P, Larkin J, et al. Improved survival with vemurafenib in melanoma with $BRAF^{V600E}$ mutation. N Engl J Med. 2011; 364:2507–2516. [PubMed: 21639808]
19. Hauschild A, Grob JJ, Demidov LV, Jouary T, Gutzmer R, Millward M, et al. Dabrafenib in *BRAF*-mutated metastatic melanoma: a multicenter, open-label, phase 3 randomised controlled trial. Lancet. 2012; 380:358–365. [PubMed: 22735384]
20. Flaherty KT, Robert C, Hersey P, Nathan P, Garbe C, Milhem M, et al. Improved survival with MEK inhibition in BRAF-mutated melanoma. N Engl J Med. 2012; 367:107–114. [PubMed: 22663011]
21. Prahallad A, Sun C, Huang S, Di Nicolantonio F, Salazar R, Zecchin D, et al. Unresponsiveness of colon cancer to $BRAF^{V600E}$ inhibition through feedback activation of EGFR. Nature. 2012; 483:100–103. [PubMed: 22281684]
22. Girotti MR, Pedersen M, Sanchez-Laorden B, Viros A, Turajlic S, Niculescu-Duvaz D, et al. Inhibiting EGF receptor or SRC family kinase signaling overcomes BRAF inhibitor resistance in melanoma. Cancer Discov. 2013; 3:158–167. [PubMed: 23242808]
23. Corcoran RB, Ebi H, Turke AB, Coffee EM, Nishino M, Cogdill AP, et al. EGFR-mediated re-activation of MAPK signaling contributes to insensitivity of BRAF mutant colorectal cancers to RAF inhibition with vemurafenib. Cancer Discov. 2012; 2:227–235. [PubMed: 22448344]
24. Dietrich S, Glimm H, Andrulis M, von Kalle C, Ho AD, Zenz T. BRAF inhibition in refractory hairy-cell leukemia. N Engl J Med. 2012; 366:2038–2040. [PubMed: 22621641]

25. Haroche J, Cohen-Aubart F, Emile JF, Arnaud L, Maksud P, Charlotte F, et al. Dramatic efficacy of vemurafenib in both multisystemic and refractory Erdheim-Chester disease and Langerhans cell histiocytosis harboring the $BRAF^{V600E}$ mutation. Blood. 2013; 121:1495–1500. [PubMed: 23258922]
26. Kuhn R, Schwenk F, Aguet M, Rajewsky K. Inducible gene targeting in mice. Science. 1995; 269:1427–1429. [PubMed: 7660125]
27. Goldman JP, Blundell MP, Lopes L, Kinnon C, Di Santo JP, Thrasher AJ. Enhanced human cell engraftment in mice deficient in RAG2 and the common cytokine receptor gamma chain. Br J Haematol. 1998; 103:335–342. [PubMed: 9827902]
28. Walter R, Schoedon G, Bachli E, Betts DR, Hossle JP, Calandra T, et al. Establishment and characterization of an arsenic-sensitive monoblastic leukaemia cell line (SigM5). Br J Haematol. 2000; 109:396–404. [PubMed: 10848831]
29. Kamata T, Pritchard CA, Leavitt AD. Raf-1 is not required for megakaryocytopoiesis and TPO-induced ERK phosphorylation. Blood. 2004; 103:2568–2570. [PubMed: 14576068]
30. Kamata T, Hussain J, Giblett S, Hayward R, Marais R, Pritchard C. BRAF inactivation drives aneuploidy by deregulating CRAF. Cancer Res. 2010; 70:8475–8486. [PubMed: 20978199]
31. Socolovsky M, Nam H-S, Fleming MD, Haase VH, Brugnara C, Lodish HF. Ineffective erythropoiesis in Stat5a(−/−)5b(−/−) mice due to decreased survival of early erythroblasts. Blood. 2001; 98:3261–3273. [PubMed: 11719363]
32. Pileri SA, Grogan TM, Harris NL, Banks P, Campo E, Chan JK, et al. Tumours of histiocytes and accessory dendritic cells: an immunohistochemical approach to classification from the International Lymphoma Study Group based on 61 cases. Histopathology. 2002; 41:1–29. [PubMed: 12121233]
33. Wilson TR, Fridlyand J, Yan Y, Penuel E, Burton L, Chan E, et al. Widespread potential for growth-factor-driven resistance to anticancer kinase inhibitors. Nature. 2012; 487:505–509. [PubMed: 22763448]
34. Straussman R, Morikawa T, Shee K, Barzily-Rokni M, Qian ZR, Du J, et al. Tumour micro-environment elicits innate resistance to RAF inhibitors through HGF secretion. Nature. 2012; 487:500–504. [PubMed: 22763439]
35. Braun BS, Shannon K. Targeting Ras in myeloid leukemias. Clin Cancer Res. 2008; 14:2249–2252. [PubMed: 18413813]
36. Chan IT, Kutok JL, Williams IR, Cohen S, Kelly L, Shigematsu H, et al. Conditional expression of oncogenic K-ras from its endogenous promoter induces a myeloproliferative disease. J Clin Invest. 2004; 113:528–538. [PubMed: 14966562]
37. Braun BS, Tuveson DA, Kong N, Le DT, Kogan SC, Rozmus J, et al. Somatic activation of oncogenic Kras in hematopoietic cells initiates a rapidly fatal myeloproliferative disorder. Proc Natl Acad Sci USA. 2004; 101:597–602. [PubMed: 14699048]
38. Wang J, Liu Y, Li Z, Du J, Ryu MJ, Taylor PR, et al. Endogenous oncogenic Nras mutation promotes aberrant GM-CSF signaling in granulocytic/monocytic precursors in a murine model of chronic myelomonocytic leukemia. Blood. 2010; 116:5991–6002. [PubMed: 20921338]
39. Lyubynska N, Gorman MF, Lauchle JO, Hong WX, Akutagawa JK, Shannon K, et al. A MEK inhibitor abrogates myeloproliferative disease in Kras mutant mice. Sci Transl Med. 2011; 3:76ra27.
40. Sabnis AJ, Cheung LS, Dail M, Kang HC, Santaguida M, Hermiston ML, et al. Oncogenic Kras initiates leukemia in hematopoietic stem cells. PLoS Biol. 2009; 7:e59. [PubMed: 19296721]
41. Van Meter ME, Díaz-Flores E, Archard JA, Passegué E, Irish JM, Kotecha N, et al. K-RasG12D expression induces hyperproliferation and aberrant signaling in primary hematopoietic stem/progenitor cells. Blood. 2007; 109:3945–3952. [PubMed: 17192389]
42. Zhang J, Wang J, Liu Y, Sidik H, Young KH, Lodish HF, et al. Oncogenic Kras-induced leukemogeneis: hematopoietic stem cells as the initial target and lineage-specific progenitors as the potential targets for final leukemic transformation. Blood. 2009; 113:1304–1314. [PubMed: 19066392]

43. Hsu CL, Kikuchi K, Kondo M. Activation of mitogen-activated protein kinase kinase (MEK)/extracellular signal regulated kinase (ERK) signaling pathway is involved in myeloid lineage commitment. Blood. 2007; 110:1420–1428. [PubMed: 17536016]

44. Blalock WL, Navolanic PM, Steelman LS, Shelton JG, Moye PW, Lee JT, et al. Requirement for the PI3K/Akt pathway in MEK1-mediated growth and prevention of apoptosis: identification of an Achilles heel in leukemia. Leukemia. 2003; 17:1058–1067. [PubMed: 12764369]

45. Shelton JG, Steelman LS, Lee JT, Knapp SL, Blalock WL, Moye PW, et al. Effects of the RAF/MEK/ERK and PI3K/AKT signal transduction pathways on the abrogation of cytokine-dependence and prevention of apoptosis in hematopoietic cells. Oncogene. 2003; 22:2478–2492. [PubMed: 12717425]

46. Heidorn SJ, Milagre C, Whittaker S, Nourry A, Niculescu-Duvas I, Dhomen N, et al. Kinase-dead BRAF and oncogenic RAS cooperate to drive tumor progression through CRAF. Cell. 2010; 140:209–221. [PubMed: 20141835]

47. Poulikakos PI, Zhang C, Bollag G, Shokat KM, Rosen N. RAF inhibitors transactivate RAF dimers and ERK signalling in cells with wild-type BRAF. Nature. 2010; 464:427–430. [PubMed: 20179705]

48. Su F, Viros A, Milagre C, Trunzer K, Bollag G, Spleiss O, et al. RAS mutations in cutaneous squamous-cell carcinomas in patients treated with BRAF inhibitors. N Engl J Med. 2012; 366:207–215. [PubMed: 22256804]

Europe PMC Funders Author Manuscripts

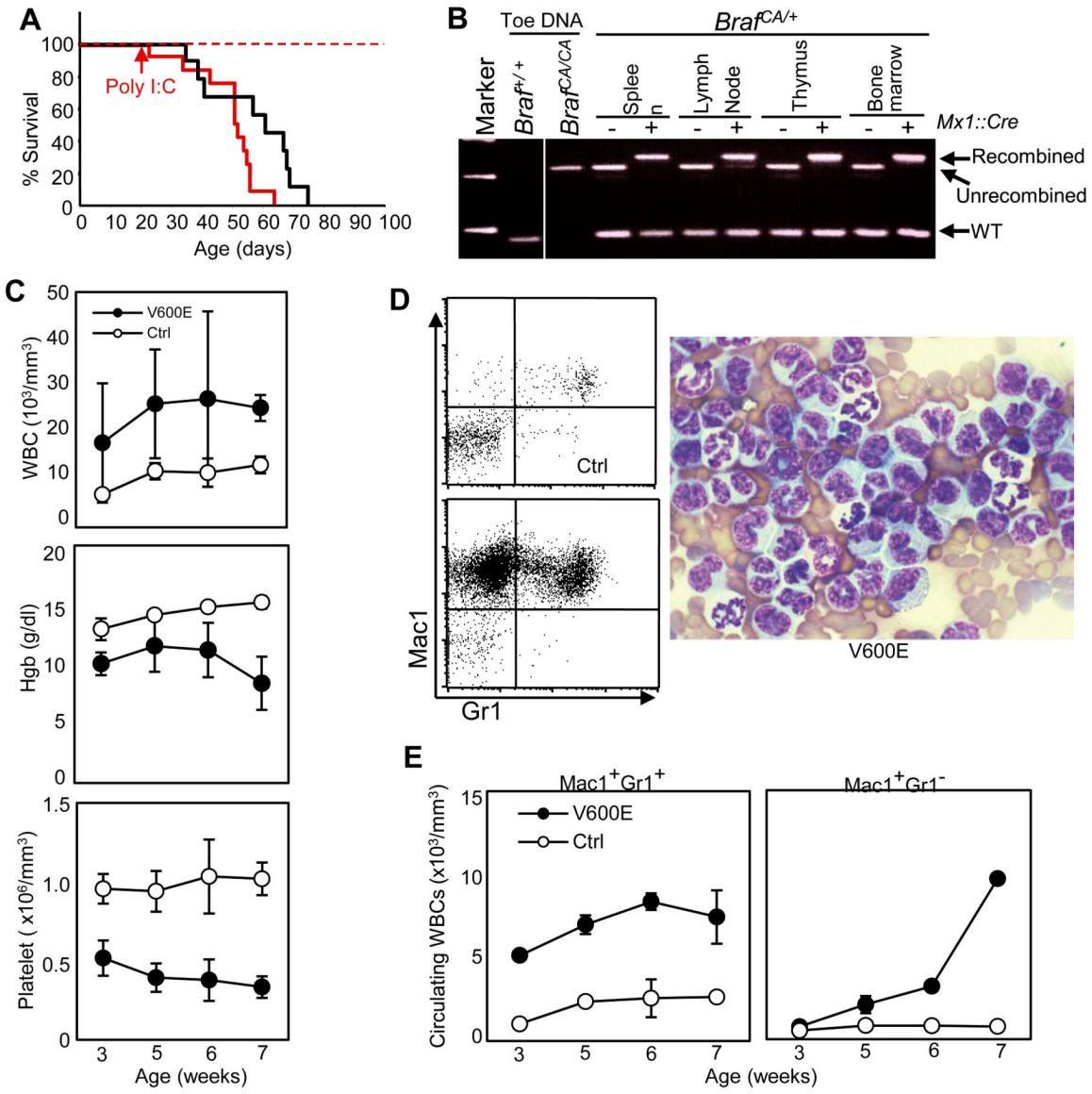

Figure 1. BRAF^{V600E} mice exibit hyperleukocytosis, anemia and thrombocytopenia

A. Percent survival of *Mx1::Cre;Braf^{CA}* (BRAF^{V600E}) mice with (red line) or without (black line) poly I:C injection at 3 weeks of age. Control *Braf$^{CA/+}$* mice lacking the *Mx1Cre* transgene with (red dashed line) or without (black dashed line) poly I:C injection served as controls. **B.** PCR detection of recombination of the *Braf^{CA}* allele in *Mx1::Cre;Braf$^{CA/+}$* hematopoietic tissues without poly I:C injection at 7 weeks of age. Unrecombined (308bp) and recombined (335bp) *Braf^{CA}* alleles, and wild-type (WT) allele (185bp) are indicated. **C.** Kinetics of circulating leukocyte counts (WBC), Hemoglobin (Hgb) concentration and platelet counts of BRAF^{V600E} (V600E) and control (Ctrl) mice from 3-7 weeks of age without poly I:C injection. **D.** Representative FACS plots for Mac1/Gr1 staining of peripheral leukocytes from poly I:C-uninjected control (Ctrl) and BRAF^{V600E} (V600E) mice (left), and a representative photograph of Giemsa-stained peripheral blood smear from poly

I:C-uninjected $BRAF^{V600E}$ mice (right) shown at x1000 original magnification. **E.** Kinetics of circulating granulocyte ($Mac1^{+}Gr1^{+}$, left) and monocyte ($Mac1^{+}Gr1^{-}$, right) counts of $BRAF^{V600E}$ (V600E) and control (Ctrl) mice from 3-7 weeks of age without poly I:C injection.

Europe PMC Funders Author Manuscripts

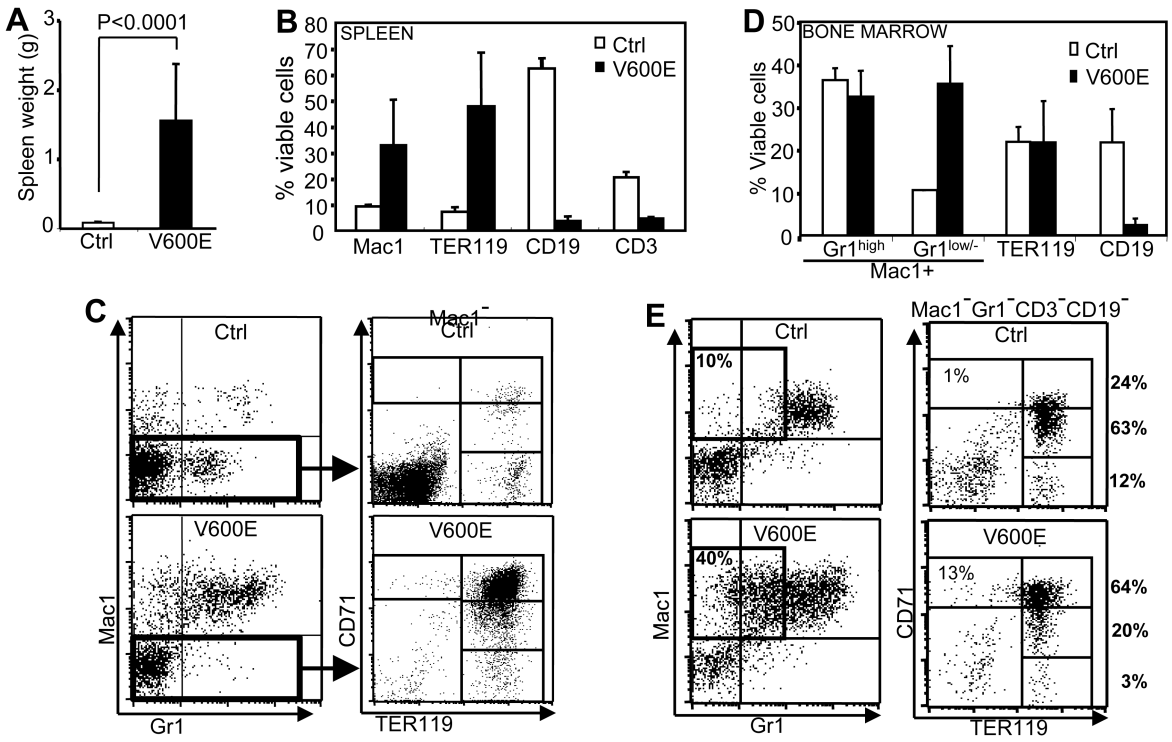

Figure 2. Spleen and bone marrow phenotypes in BRAF^{V600E} mice

A. Spleen weights of control (Ctrl) and BRAF^{V600E} (V600E) mice. **B.** Flow cytometry quantification of relative percentages of splenic myeloid (Mac1^{+}), erythroid (TER119^{+}), B-lymphoid (CD19^{+}) and T-lymphoid (CD3^{+}) cells in poly I:C uninjected BRAF^{V600E} (V600E) and control (Ctrl) mice. **C.** Representative flow cytometry plots of spleen cells from BRAF^{V600E} (V600E) or control (Ctrl) mice. Mac1/Gr1 plots of nucleated cells (left) and CD71/TER119 plots of Mac1-negative cells (right) are indicated. **D**. Flow cytometry quantification of relative percentages of Mac1^{+}Gr1^{high} (granulocytes), Mac1^{+}Gr1$^{low/-}$ (monocytes), TER119^{+} (erythroid) and CD19^{+} (B-lymphocytes) populations in bone marrow of BRAF^{V600E} (V600E) and control (Ctrl) mice. **E**. Representative flow cytometry plots of bone marrow nucleated cells from BRAF^{V600E} (V600E) and control (Ctrl) mice. Mac1/Gr1 plots (left) highlight the Mac1^{+}Gr1$^{low/-}$immature monocytic cell population, and CD71/TER119 plots of Mac1^{-}/Gr1^{-}/CD3^{-}/CD19^{-} cells (right) highlight erythroid populations with CD71^{+}TER119^{-}, CD71^{+}TER119^{+}, CD71^{dim}TER119^{+} or CD71^{-}TER119^{+} phenotype. The percentage of each population in total erythroid cells is indicated. All data are from mice not injected with polyI:C.

Europe PMC Funders Author Manuscripts

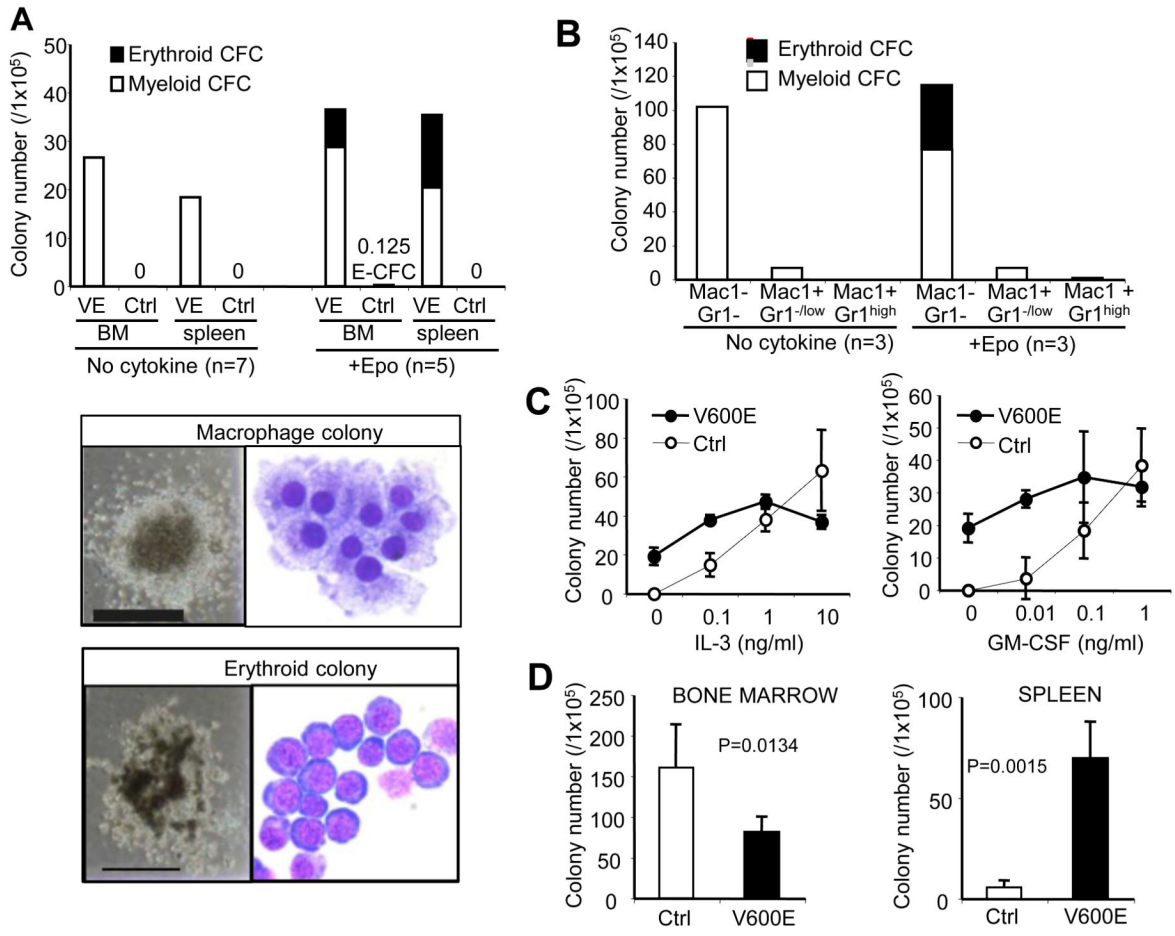

Figure 3. *In vitro* charactrerization of BRAF^{V600E} hematopoietic progenitors

A. **(Top)** myelo-erythroid colony formation of BRAF^{V600E} (VE) and control (Ctrl) bone marrow and spleen cells in cytokine-free or Epo-added mechylcellulose cultures (average of 5-7 independent experiments). **(Bottom)** Representative images of the cytokine-independent macrophage colony (top) and the Epo-dependent erythroid colony (bottom). Phase-constrast microphotographs (shown at x40 original magnification, grid: 2mm) and Giemsa-staining of cytospin preparations (shown at x1000 original magnification) are indicated. **B**. Myelo-erythroid colony formation of the sorted Mac1^{-}Gr1^{-}, Mac1^{+}Gr1$^{-/low}$, and Mac1^{+}Gr1^{high} BRAF^{V600E} bone marrow populations in cytokine-free or Epo-added mechylcellulose culture (average of 3 independent experiments). **C**. Myeloid colony development of control (Ctrl) and BRAF^{V600E} (V600E) bone marrow cells in the presence of increasing concentrations of IL-3 (0.1-10ng/ml, left) or GM-CSF (0.01-1ng/ml, right). **D**. Myeloid colony numbers generated from 1×10^{5} bone marrow (left) or spleen (right) cells from BRAF^{V600E} (V600E) or control (Ctrl) mice in the presence of IL-3 (10ng/ml), SCF (50ng/ml), EPO (4U/ml) and TPO (100ng/ml).

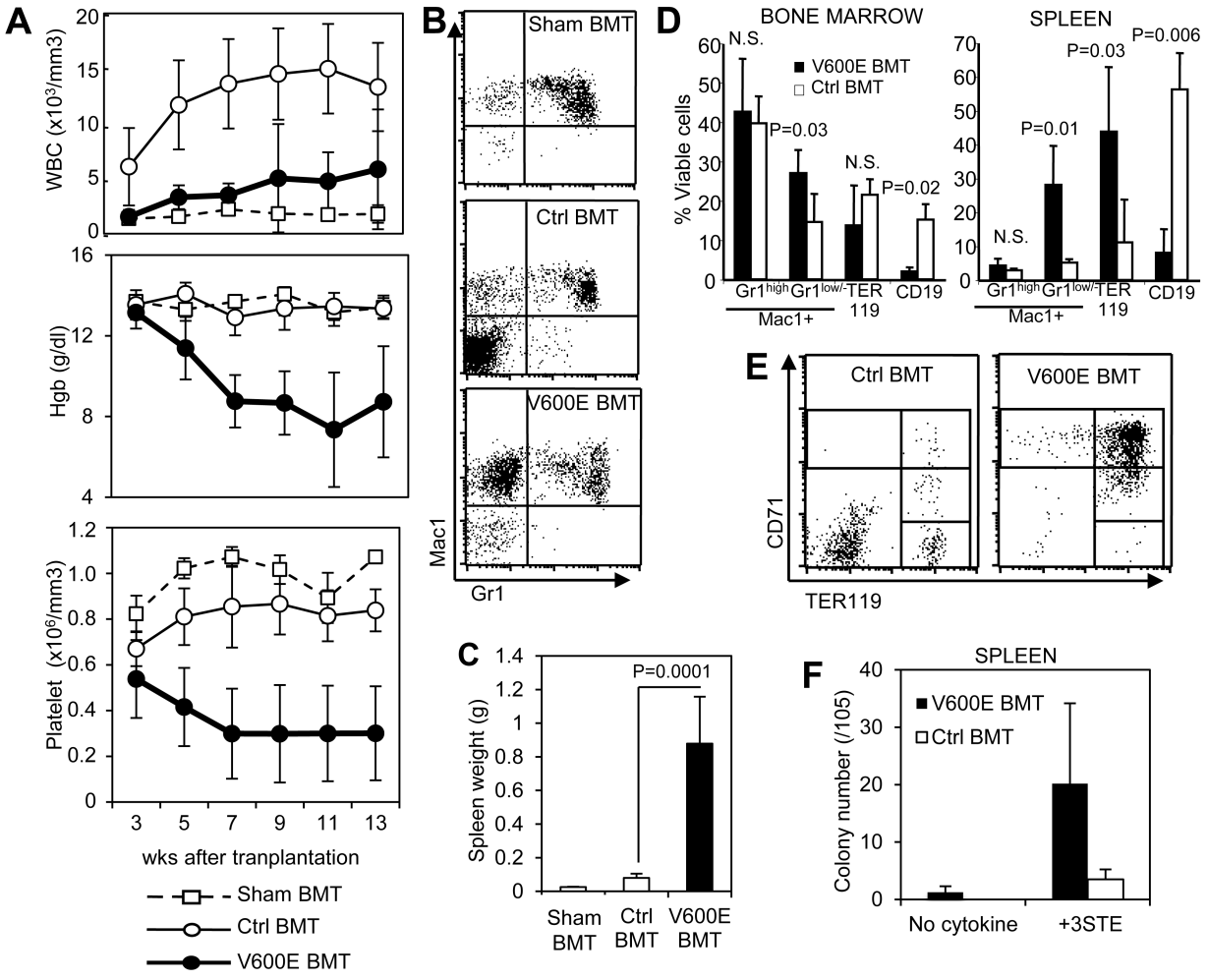

Figure 4. Transplantation of BRAF^{V600E} bone marrow in sublethally-irradiated recipients

A. Kinetics of circulating leukocyte counts (top), hemoglobin values (middle) and platelet counts (bottom) of sub-lethally-irradiated *Rag2*$^{-/-}\gamma c^{-/-}$ mice transplanted with 2×10^6 bone marrow cells from BRAF^{V600E} mice (V600E BMT; filled circles, n=14) or control mice (Ctrl BMT; open circles, n=9), or injected with PBS only (Sham BMT; open squares, n=3). Peripheral blood was monitored at 3, 5, 7, 9, 11 and 13 weeks after transplantation. **B**. Representative Mac1/Gr1 FACS plots of circulating leukocytes in the recipients injected with PBS (Sham BMT, top) or transplanted with control (Ctrl BMT, middle) or BRAF^{V600E} (V600E BMT, bottom) bone marrow. **C**. Spleen weights in the recipients injected with PBS (Sham BMT), control bone marrow (Ctrl BMT) or BRAF^{V600E} bone marrow (VE BMT) at 10-13 weeks after transplantation. **D**. Flow cytometry quantification of Mac1$^+$Gr1^{high} (granulocytes), Mac1$^+$Gr1$^{low/-}$ (monocytes), TER119$^+$ (erythroid) and CD19$^+$ (B-lymphocytes) populations in bone marrow (top) and spleen (bottom) of control (Ctrl BMT) or BRAF^{V600E} (V600E BMT) bone marrow recipients at 10-13 weeks after transplantation. P-values by student's *t*-test are indicated. **E**. Representative CD71/TER119 FACS plots of Mac1-negative spleen cells in control (Ctrl BMT) or BRAF^{V600E} (V600E BMT) bone marrow recipients. **F**. Myeloid colony formation of spleen cells from control (Ctrl BMT) or BRAF^{V600E} (V600E BMT) bone marrow recipients in mechylcellulose media with or

Europe PMC Funders Author Manuscripts

without multiple cytokines (as in Figs. 3A and D). Data in D and F represent mean +/− SD (n=6 for V600E, n=3 for Ctrl).

Europe PMC Funders Author Manuscripts

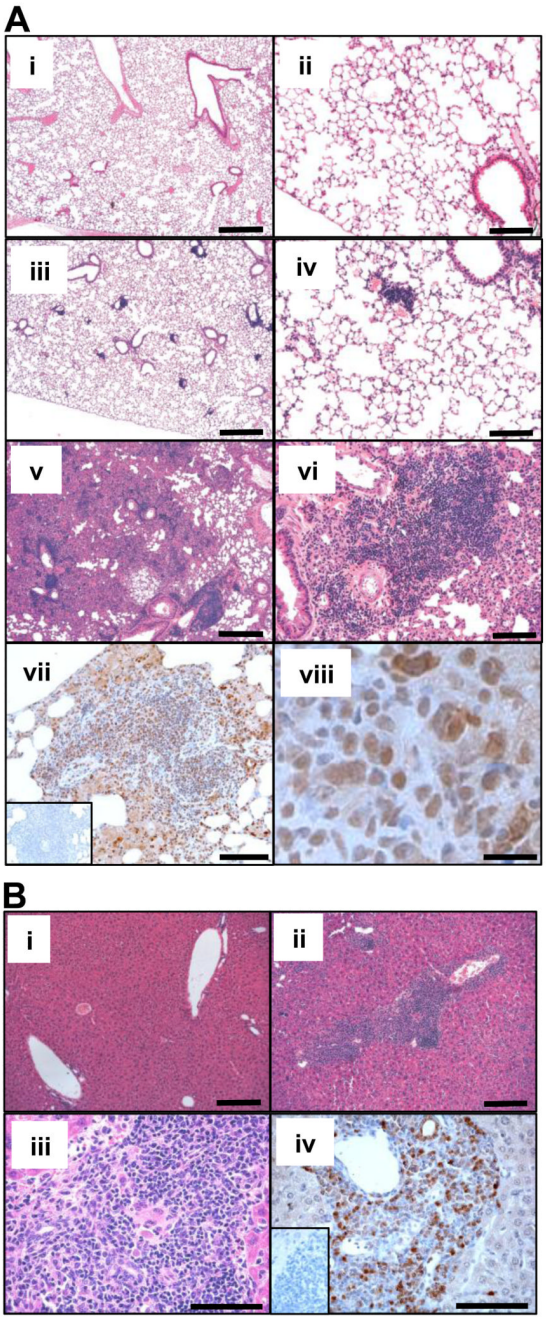

Figure 5. Pulmonary and hepatic involvement in BRAF^{V600E} bone marrow recipients

A. H&E (i-vi) and S100 (vii-viii) staining of the lungs of bone marrow recipients. Tissue sections from sham (i-ii), control marrow (iii-iv), and BRAF^{V600E} marrow recipients (v-viii) are shown at x50 (I, iii and v), x200 (ii, iv, vi and vii) or x1000 (viii) original magnification. Scale bars: 500mm for (i), (iii), (v); 125mm for (ii), (iv), (vi), (vii); 20mm for (viii) **B**. H&E (i-iii) and S100 (iv) staining of the livers of control (i) and BRAF^{V600E} (ii-iv) marrow recipients, shown at x100 (i-ii) or x400 (iii-iv) original magnification. Inset figures (A-vii and B-iv) show negative control staining prepared by omitting the primary antibody. Scale bars: 250mm for (i), (ii); 100mm for (iii), (iv)

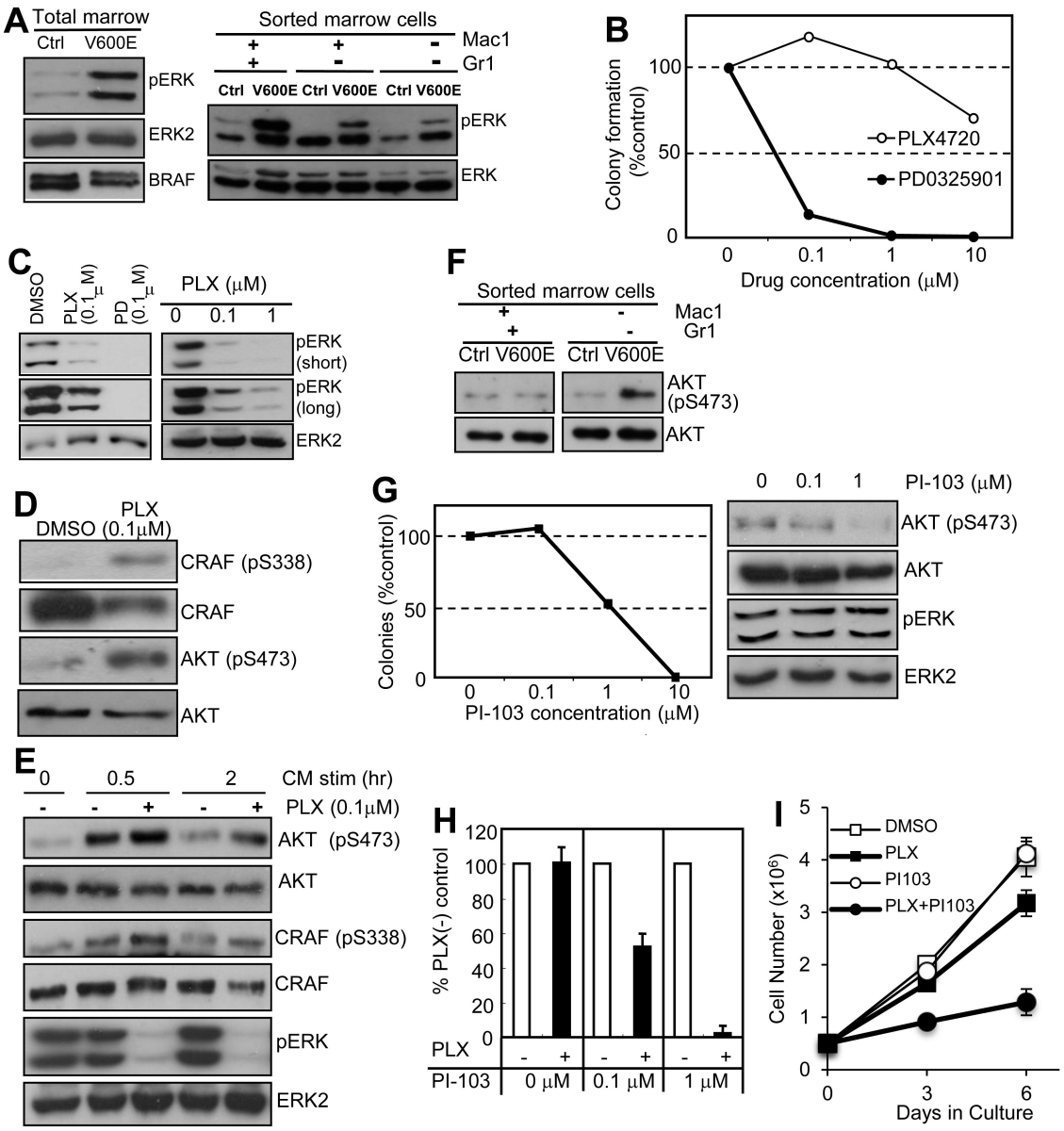

Figure 6. Functional and biochemical characterization of PLX-resistance

A. ERK phosphorylation characterized in total and sorted primary bone marrow cells from control (Ctrl) and $BRAF^{V600E}$ (V600E) mice. **B**. Cytokine-independent colony formation of $BRAF^{V600E}$ bone marrow cells in the presence of 0-10μM PD0325901 (filled circles) or PLX4720 (open circles). The average of two independent experiments indicated. **C**. Phospho-ERK immunoblots of the lysates of $BRAF^{V600E}$ bone marrow cultures treated with 0.1μM PLX4720 (PLX) or PD0325901 (PD) (left), or with 0-1μM PLX4720 (right), for 24hrs in a serum-free condition. **D**. Phospho-CRAF (S338) and AKT (S473) immunoblots of the lysates of $BRAF^{V600E}$ bone marrow cultures treated with 0.1μM PLX4720 or vehicle (DMSO) for 24hrs in a serum-free condition. **E**. Phospho-CRAF (S338), AKT (S473) and ERK immunoblots of the lysates of $BRAF^{V600E}$ bone marrow cultures stimulated for 0.5-2

hrs with the CM (with DMSO) or 0.1μM PLX4720 after 5hrs serum starvation. **F**. AKT phosphorylation (S473) of the sorted $Kit^{+}Mac1^{-}Gr1^{-}$ bone marrow cells from control (Ctrl) and $BRAF^{V600E}$ (V600E) mice. **G**. Cytokine-independent colony formation of $BRAF^{V600E}$ bone marrow cells in the presence of 0-10μM PI-103 (left, average of two independent experiments), and phospho-AKT (S473) immunoblots of the lysates of $BRAF^{V600E}$ bone marrow cultures treated with 0-1μM PI-103 for 96hrs in a serum-free condition (right). **H**. Cytokine-independent colony formation of $BRAF^{V600E}$ bone marrow cells in methylcellulose media containing 0.1μM PLX4720 (PLX) in the presence of 0, 0.1, or 1 μM PI-103, normalized to the vehicle control culture at each PI-103 concentration (% PLX(-) conrtol). Data indicate the average +/− SD of three independent experiments. **I**. SigM5 growth curves with cells grown in: DMSO (control), PLX4720 0.1μM (PLX), PI-103 0.1μM (PI103), and PLX4720 0.1μM + PI-103 0.1μM (PLX+PI103). Data indicate the average +/− SD of three independent experiments

Table 1

Bone marrow progenitor colony formation and chimerism in transplant recipients.

Recipient mouse#	Colony #/10^5 BM cells		Chimerism (+3STE)[c]		
	No cytokine	+3STE[b]	% Donor chimerism	Recipient CFU# /10^5	Donor CFU# /10^5
$BRAF^{V600E}$ BMT[a]					
103	0	85	6.7	79.3	5.7
106	9	92.5	6.7	86.3	6.2
114	31	42.5	53.3	19.8	22.7
118	15	117.5	0	117.5	0
122	9	80	15.4	67.7	12.3
127	33.5	72.5	93.3	4.8	67.7
Average	**16.3**	**81.7**	**29.2**	**62.6**	**19.1**
Control BMT [a]					
116	0	165	46.7	88	77
124	0	190	26.7	139.3	50.7
128	0	225	53.3	105	120
Average	**0**	**193.3**	**42.2**	**110.8**	**82.6**

[a] 2×10^6 bone marrow nucleated cells from $BRAF^{V600E}$ or control mice 3 weeks after poly I:C injection were injected into each sublethally (5 Gy) irradiated *Rag2*$^{-/-}\gamma c^{-/-}$ recipient.

[b] 10ng/ml IL-3, 50ng/ml SCF, 100ng/ml TPO and 4U/ml EPO were added in "+3STE" cultures.

[c] Donor chimerism was determined by *Braf* genotyping of randomly plucked individual colonies developed in "+3STE" cultures, and CFU# of donor or recipient origin was calculated by multiplying total colony numbers by the %chimerism.